BIOCHEMISTRY
including biophysical chemistry & molecular biology
Article

Biochemistry **2009,** *48,* 11421–11431 11421
DOI: 10.1021/bi901438z

Assembly with the Na,K-ATPase α_1 Subunit Is Required for Export of β_1 and β_2 Subunits from the Endoplasmic Reticulum[†]

Elmira Tokhtaeva, George Sachs, and Olga Vagin*

Department of Physiology, School of Medicine, UCLA and Veterans Administration Greater Los Angeles Health Care System, Los Angeles, VAGLAHS/West LA, Building 113, Room 324, 11301 Wilshire Boulevard, Los Angeles, California 90073

Received August 16, 2009; Revised Manuscript Received September 16, 2009

ABSTRACT: The level of the heterodimeric Na,K-ATPase is tightly controlled in epithelia to maintain appropriate transport function. The catalytic Na,K-ATPase α subunit is not able to exit the ER or catalyze ion transport unless assembled with the β subunit. However, requirements for the ER exit of the Na,K-ATPase β subunit that plays an additional, ion-transport-independent, role in intercellular adhesion are not clear. Exogenous β_1 or β_2 subunits expressed in renal MDCK cells replace endogenous β_1 subunits in the $\alpha-\beta$ complexes in the ER, resulting in a decrease in the amount of the α_1-bound endogenous β_1 subunits by 47−61% with no change in the amount of α_1 subunits. Disruption of the $\alpha_1-\beta$ association by mutations in defined α_1-interacting regions of either β_1 or β_2 subunits results in the ER retention and rapid degradation of unassembled mutants. Hence, the ER quality control system allows export only of assembled $\alpha-\beta$ complexes to the Golgi, thereby maintaining an equimolar ratio of α and β subunits in the plasma membrane, whereas the number of α_1 subunits in the ER determines the amount of the $\alpha-\beta$ complexes.

The sodium pump is expressed in all animal tissues where it establishes concentration gradients for Na^+ and K^+ by pumping three Na^+ from the cytoplasm in exchange for two extracellular K^+. The ion gradients generated by the Na,K-ATPase are used in many essential cellular processes, such as osmoregulation, generation of plasma membrane potential and maintenance of intracellular pH and Ca^{2+} concentration, vectorial transport of many solutes, and excitability in muscle fibers and neurons. Further, the Na,K-ATPase serves as a functional signal transducer (*1*, *2*).

The pump is a heterodimer, consisting of an α subunit that is responsible for ion transport and a β subunit that is implicated in maturation and membrane targeting of the enzyme. There are four isoforms of the Na,K-ATPase α subunit (α_1, α_2, α_3, and α_4) and three isoforms of the Na,K-ATPase β subunit (β_1, β_2, and β_3) (*3*, *4*). Additional tissue-specific regulatory subunits of the Na,K-ATPase that belong to the FXYD family of small membrane proteins have also been identified (*5*). Most data have shown that α and β subunits are always present in equimolar amounts in the isolated Na,K-ATPase (*6*−*9*). Recent data claiming that the $\alpha-\beta$ ratio can be less (*10*) or more (*11*) than one are difficult to reconcile with the 3D high-resolution structure of the enzyme that shows two specific regions of interaction between the α and β subunits at a 1:1 stoichiometry (*12*, *13*). Given these sites of interaction, stable recruitment of additional β subunits to the α subunit or vice versa is unlikely.

ER assembly of the α with the β subunit is necessary for export of the α subunit of the Na,K-ATPase from the ER to the Golgi and formation of functional enzyme (*14*), suggesting that the β subunit acts as a molecular chaperone that facilitates maturation of the enzyme (*15*, *16*).

In addition, both β_1 and β_2 subunits have important nonenzymatic roles such as formation and maintenance of intercellular junctions and regulation of cell migration (*16*−*23*). It is not known whether the β subunits perform these functions only as components of the $\alpha-\beta$ complexes or perhaps as individual plasma membrane proteins.

Results of studies addressing the question as to whether unassembled β subunits are present in the plasma membrane are ambiguous. A consecutive series of immunoprecipitation using the antibody against the α_1 subunit resulted in depletion of MDCK cell lysates of the mature but not immature β_1 subunits, indicating that the mature β_1 subunits are all bound to the α_1 subunit (*10*). Along with these data, overexpressed *Xenopus* oocyte Na,K-ATPase β_1 and β_3 subunits are retained in the ER in the absence of the α subunit in *Xenopus* oocytes (*24*−*26*). By contrast, the *Torpedo californica* β_1 subunit expressed in *Xenopus* oocytes without the α subunit shows the mature N-glycosylation pattern, implying that it is able to traffic from the ER to the Golgi (*27*). Whether the unassembled Na,K-ATPase β_2 subunit isoform is able to reach the plasma membrane is unknown. However, the H,K-ATPase β subunit that has more homology with the Na,K-ATPase β_2 subunit than the other Na,K-ATPase β subunit isoforms is detected in the plasma membrane when expressed without the H,K-ATPase α subunit in various cell types (*28*−*32*).

In this work, analysis of the nature of the N-linked glycans of endogenous and expressed β subunits of the Na,K-ATPase enables determination of their localization either in the ER or in the post-ER compartments. The presence of high-mannose-type N-glycans shows ER location of the β subunits, while the presence of hybrid- or complex-type N-glycans in the β subunits that can only be generated by Golgi-located glycosyltransferases shows successful export of the β subunits from the ER. Renal MDCK cells were used as an expression system for YFP-linked

[†]Supported by NIH Grants DK077149 and DK058333.
*Corresponding author. E-mail: olgav@ucla.edu. Phone: 310-268-3924. Fax: 310-312-9478.

Published on Web 09/18/2009

β_1 and β_2 subunit isoforms and β subunit mutants in order to determine whether assembly with the α subunit is essential for ER exit of either β_1 or β_2 subunits. Confocal microscopy, immunohistochemistry, immunoprecipitation, surface-selective biotinylation, and Western blot analysis were employed to evaluate trafficking and molecular interactions of endogenous and exogenous Na,K-ATPase subunits. The results show that (i) association with the α subunit at 1:1 stoichiometry is a prerequisite for the export of both the β_1 and β_2 subunits from the ER and (ii) the amount of the α subunit in the ER is a limiting factor for α−β assembly.

MATERIALS AND METHODS

Construction of MDCK Stable Cell Lines. The fusion proteins with YFP linked to the N-terminus of the Na,K-ATPase rat β_1 or human β_2 subunit (YFP-β_1[1] and YFP-β_2) were constructed as described previously (*23*). Y39A/F42A/Y43A (YFY/AAA) and P245G (P/G) mutants of YFP-β_1 and homologous Y44A/F47A/Y48A (YFY/AAA) and P229G (P/G) mutants of YFP-β_2 were constructed by site-directed mutagenesis using the QuikChange mutagenesis kit (Stratagene). The homologous residues in the rat β_1 or human β_2 subunits were determined based on the computational alignment (Supporting Information Figure 1). The mutagenic primers (Supporting Information Table 1) were constructed using PrimerSelect software, 5.03. Stable MDCK cell lines expressing wild-type and mutated YFP-β_1 and YFP-β_2 were obtained as described previously (*33*).

The fusion protein with YFP linked to the N-terminus of the dog Na,K-ATPase β_1 subunit was constructed by cloning a cDNA encoding dog Na,K-ATPase β_1 subunit into a multicloning site of pEYFP-C1 (Clontech) using *Kpn*I and *Bam*HI restriction sites. Then, the stop codon was removed in the linker between YFP and Na,K-ATPase β_1 subunit by site-directed mutagenesis. A cDNA encoding dog Na,K-ATPase β_1 subunit was obtained from $pCIN_4$ vector, a kind gift from Liora Shoshani.

Cell Culture. Cells were grown in DMEM medium (Cellgro Mediatech) containing 4.5 g/L glucose, 2 mM L-glutamine, 8 mg/L phenol red, 100 units/mL penicillin, 0.1 mg/mL streptomycin, and 10% FBS. Where indicated, 2 μg/μL swainsonine (Sigma), 100 μg/mL deoxymannojirimycin (Sigma), or 20 μg/mL cycloheximide (Sigma) was added to the cell culture medium.

Confocal Microscopy. Confocal microscopy images were acquired using the Zeiss LSM 510 laser scanning confocal microscope and LSM 510 software, version 3.2.

Primary Antibodies. The following monoclonal antibodies were used for immunoprecipitation, immunostaining, and Western blot analysis: against the Na,K-ATPase α_1 subunit, clone C464.6 (Millipore); against GFP, clones 7.1 and 13.1, that also recognize YFP (Roche Diagnostics). Also, polyclonal antibodies against the Na,K-ATPase α_1 subunit (Cell Signaling) and against GFP that also recognize YFP (Clontech) were used.

Immunofluorescent Staining of MDCK Cells. Cells were fixed by incubation with 3.75% formaldehyde in PBS for 15 min at 37 °C and permeabilized by incubation with 0.1% Triton X-100 for 5 min. Then cells were incubated with Dako protein block serum-free solution (Dako Corp.) for 30 min. Immunostaining of the Na,K-ATPase α_1 subunit was performed by 1 h incubation with the monoclonal antibody against the Na,K-ATPase α_1 subunit followed by 1 h incubation with Alexa Fluor 633 conjugated anti-mouse antibody (Invitrogen).

Transient Transfection of MDCK Cells with the Fluorescent Marker of the ER. Cells grown on glass-bottom microwell dishes (MatTek Corp.) were transfected with the plasmid encoding a fusion protein between *Discosoma* sp. red fluorescent protein and the marker of the ER, DsRed2-ER (Clontech), using the Lipofectamine 2000 transfection reagent (Invitrogen) according the manufacturer's instructions. Confocal microscopy images of transfected cells were acquired 24−48 h after transfection.

Immunoprecipitation. Monolayers of MDCK cells grown in a 35 mm^2 well of a six-well plate were rinsed twice with ice-cold PBS and lysed by incubation with 200 μL of 150 mM NaCl in 50 mM Tris, pH 7.5, containing 1% Nonidet P40, 0.5% sodium deoxycholate, and Complete protease inhibitor cocktail, 1 tablet/50 mL (Roche Diagnostics). Cell extracts were clarified by centrifugation (15000*g*, 10 min) at 4 °C. Then, the cell extracts were incubated with 30 μL of the protein A−agarose suspension (Roche Diagnostics) in a total volume 1 mL of the lysis buffer at 4 °C with continuous rotation for at least 3 h (or overnight) to remove the components that nonspecifically bind to protein A. Precleared supernatant was mixed with 3 μL of the polyclonal anti-YFP antibody or 20 μL of the polyclonal antibody against the Na,K-ATPase α_1 subunit and incubated with continuous rotation at 4 °C for 60 min. After addition of 30 μL of the protein A−agarose suspension, the mixture was incubated at 4 °C with continuous rotation overnight. The bead-adherent complexes were washed three times on the beads, and then proteins were eluted from the beads by incubation in 35 μL of SDS−PAGE sample buffer (4% SDS, 0.05% bromophenol blue, 20% glycerol, 1% β-mercaptoethanol in 0.1 M Tris, pH 6.8) for 5 min at 80 °C.

Isolation of Basolateral Plasma Membrane Proteins of MDCK Cells Using Surface-Specific Biotinylation. Cells were maintained for 6 days after becoming confluent in transwell inserts. Biotinylation of surface proteins was performed according to previously described procedures (*34*, *35*). Cell monolayers were biotinylated with EZ-Link sulfo-NHS-SS-biotin (Pierce) that was added into the well only (basolateral surface of the tight cell monolayers). After quenching the biotinylation reaction, cells were washed and then lysed by incubation with 200 μL of 0.15 M NaCl in 15 mM Tris, pH 8.0, with 1% Triton X-100 and 4 mM EGTA. Cell extracts were clarified by centrifugation (15000*g*, 10 min) at 4 °C. To isolate surface biotinylated proteins, the cell extract was incubated with 100 μL of streptavidin−agarose beads (Sigma-Aldrich) in a total volume of 1 mL of 0.15 M NaCl in 15 mM Tris, pH 8.0, with 0.5% Triton X-100 and 4 mM EGTA at 4 °C with continuous rotation for 60 min. The bead-adherent complexes were washed three times on the beads, and then proteins were eluted from the beads by incubation in 40 μL of SDS−PAGE sample buffer for 5 min at 80 °C.

Western Blot Analysis of the Total and Immunoprecipitated Proteins of MDCK Cells. Samples containing 7−8 μg of protein in 10 μL of the MDCK cell extract mixed with 10 μL of SDS−PAGE sample buffer, or immunoprecipitated proteins eluted from the protein A/G-conjugated agarose beads, or basolateral biotinylated proteins eluted from streptavidin−agarose beads were loaded onto 4−12% gradient SDS−PAGE gels (Invitrogen). Proteins were separated by SDS−PAGE using MES/SDS running buffer (0.05 M MES, 0.05 M

[1]Abbreviations: YFP-β_1 and YFP-β_2, the fusion proteins between the yellow fluorescent protein and the Na,K-ATPase β_1 subunit and β_2 subunit, respectively.

Tris base, 0.1% SDS, and 1 mM EDTA, pH 7.3), transferred onto a nitrocellulose membrane (Bio-Rad), and detected by Western blot analysis using the appropriate primary antibody and the anti-mouse or anti-rabbit IgG conjugated to alkaline phosphatase (Promega) as a secondary antibody. Alkaline phosphatase was detected using nitro blue tetrazolium and 5-bromo-4-chloro-3-indolyl phosphate in alkaline phosphatase buffer (150 mM NaCl and 1 mM $MgCl_2$ in 10 mM Tris-HCl, pH 9.0). Immunoblots were quantified by densitometry using Zeiss LSM 510 software, version 3.2.

RT Real-Time Quantitative Polymerase Chain Reaction. Total RNA from MDCK cells was isolated using RNAqueous (Ambion). Typical RNA concentrations were 100−200 ng/μL. The RNA was measured for purity and stability with a Bioanalyser 2100 (Agilent Technologies). Total RNA (2000 ng) in total 40 μL volume was converted to cDNA by use of the Omniscript RT kit (Qiagen) and an oligo$(dT)_{12-18}$ primer (Invitrogen), according to the manufacturer's protocol. One microliter of RT product was amplified by real-time PCR using the SYBR premix ExTaq perfect real-time PCR kit (TaKaRa), according to the manufacturer's protocol. The primers used are shown in Supporting Information Table 2. Real-time PCR was performed in eight-well strips using a DNA Engine Opticon 2 (MJ Research). The cycle of threshold (C_t) was determined for each primer set. The efficiency of amplification was determined by generating a standard curve for each primer pair using a corresponding PCR product as a template. The PCR products were purified by using the MinElute gel extraction kit (Qiagen). The range of PCR product concentrations was chosen for each primer set so that the standard curve included the values of C_t observed for the RNA samples isolated from both nontransfected and transfected cells. The resulting values of C_t were plotted against the logarithm of the PCR product copy number. Quantification of the mRNA levels was performed as described previously (*22*) using the β-actin mRNA as a reference. All reactions were carried out in duplicate, and three separate mRNA isolations were performed.

Trypsin Digestion. Susceptibility of the mutated and wild-type Na,K-ATPase β subunits to limited tryptic digestion was used to assess the effect of mutations on folding of the subunit. In order to prevent heterogeneity in N-glycan sizes, cells were treated with 100 μg/mL deoxymannojirimycin, α-mannosidase I inhibitor, for 48 h prior to the trypsin digest experiment. Deoxymannojirimycin prevents synthesis of both complex- and hybrid-type N-linked oligosaccharide chains; as a result, all newly synthesized N-glycans become high-mannose type. Incubation with the inhibitor for 48 h was found to be sufficient to replace the vast majority of the existing YFP-linked β subunits by newly synthesized high-mannose-type glycosylated forms of the subunits.

The monolayers of deoxymannojirimycin-treated cells were rinsed twice with ice-cold PBS and lysed by incubation with 200 μL of 150 mM NaCl in 50 mM Tris, pH 7.5, containing 1% Nonidet P40 and 0.5% sodium deoxycholate. Protein concentration in cell lysates was determined using the BCA assay kit (Pierce) and adjusted to 2.3 mg/mL. Cell lysates were incubated with trypsin, which was added in the range of 0−3 μg/mL as indicated at 37 °C for 30 min. The reaction was stopped by the addition of 20 μg/mL soy trypsin inhibitor (Sigma-Aldrich) and incubation of samples on ice for 10 min. Then, samples containing 10 μL of reaction mixture combined with 10 μL of SDS−PAGE sample buffer were incubated at 80 °C for 5 min, subjected to 4−12% SDS−PAGE, and analyzed by Western blotting by using a monoclonal anti-YFP antibody.

Glycosidase Cleavage. Where indicated, the total cell lysates were treated with EndoH from *Streptomyces plicatus* (GlycoProzyme Inc.) according to the manufacturer's instructions.

Statistical analysis was performed using Student's *t* test (GraphPad Prism 4 software and Microsoft Excel). Statistical significance is specified in the figure legends.

RESULTS

The High-Mannose Forms of Endogenous and Exogenous Na,K-ATPase β Subunits Reside in the ER. In MDCK cells, the major endogenous Na,K-ATPase subunit isoforms are α_1 and β_1. The endogenous β_1 subunit contains two N-glycosylated forms that are detected as a broad band at 45−55 kDa and a sharper band at ~40 kDa (Figure 1B, bands M and I, respectively). Only the top band is found in the basolateral plasma membrane (Figure 3A, central panel), showing that the lower band represents the intracellular immature fraction of the subunit and the higher band represents the mature plasma membrane form.

The mature form of the β_1 subunit is resistant to EndoH digestion, while the immature form is digested by EndoH producing the deglycosylated form of the β_1 subunit (Figure 1B, right panel). EndoH cleaves hybrid- or high-mannose-type N-glycans but not the complex-type N-glycans from the glycoproteins (Figure 1A). Therefore, the mature form of the β_1 subunit contains only complex-type N-glycans, whereas N-glycans of the immature form are either hybrid or high-mannose type, or a mixture of the two types.

To further define the type of the N-glycans of the intracellular fraction of β_1 subunit, MDCK cells were incubated with inhibitors of N-glycan processing such as swainsonine and deoxymannojirimycin that preserve the hybrid type or high-mannose type of N-glycans, respectively (Figure 1A). The electrophoretic mobility of the immature form of the β_1 subunit in the control cells is similar to the mobility of the β_1 subunit in deoxymannojirimycin-treated cells but greater than that in swainsonine-treated cells (Figure 1B, left and central panels), showing that N-glycans of the immature form are actually high-mannose but not hybrid type. Similarly, expressed YFP-β_1 and YFP-β_2 contain mature and immature forms. Experiments with deoxymannojirimycin showed that N-glycans of the immature forms of YFP-β_1 and YFP-β_2 are also of the high-mannose type (Supporting Information Figure 2).

High-mannose-type N-glycans are added to glycoproteins cotranslationally in the ER. Although processing of N-glycans starts immediately after their covalent linkage to the asparagines of N-glycosylation sites, all N-glycans preserve the high-mannose structure while they reside in the ER. Only after export of the β subunit to the Golgi are the high-mannose N-glycans transformed to hybrid- and complex-type glycans due to the action of Golgi-located mannosidases and glycosyltransferases (Figure 1A). Since the immature forms of the β subunits are high-mannose but not hybrid type, they must reside in the ER.

Therefore, the relative content of the high-mannose form of the β subunit in whole cell lysates quantitatively reflects the fraction of the β subunits present in the ER. Similarly, the relative content of the high-mannose form of the β subunit in the α_1-coprecipitated fractions reflects the ER-located portion of the α_1-assembled β subunits prior to their export to the Golgi.

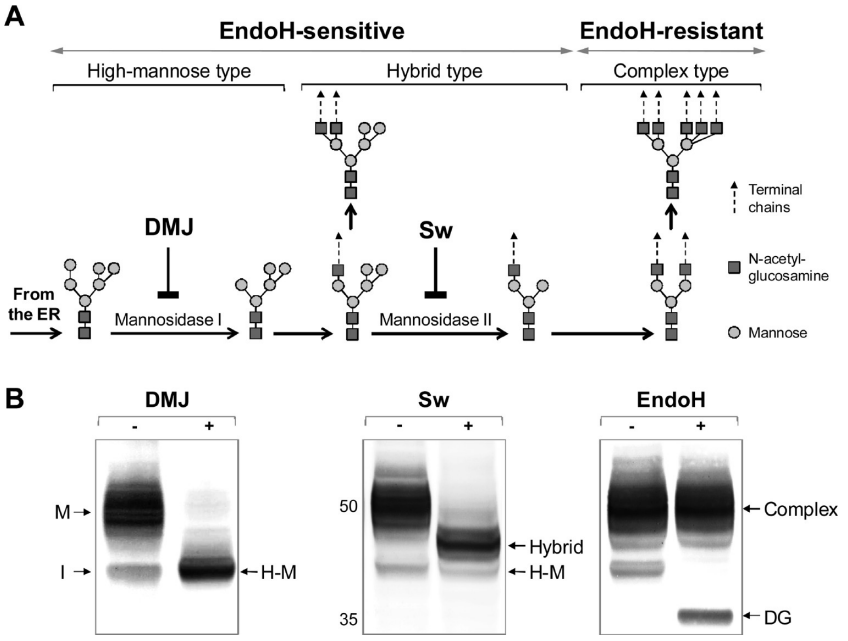

FIGURE 1: The N-glycans of the immature form of the endogenous Na,K-ATPase β_1 subunit are high-mannose type. (A) A simplified scheme showing transformation of high-mannose N-glycans into hybrid- and complex-type N-glycans in the Golgi. The Golgi mannosidases I and II remove terminal mannose residues allowing covalent addition of *N*-acetylglucosamine residues followed by branching and elongation of N-glycans due to the action of various Golgi glycosyltransferases. A specific inhibitor of the Golgi mannosidase I, deoxymannojirimycin (DMJ), prevents formation of both hybrid- and complex-type N-glycans, thus preserving the high-mannose type structure of N-glycans. A specific inhibitor of the Golgi mannosidase II, swainsonine (Sw), prevents transformation of hybrid-type N-glycans into complex-type N-glycans. Endoglycosidase EndoH can be used as a tool to distinguish the complex-type N-glycans that are resistant to the action of this enzyme from the EndoH-cleavable high-mannose and hybrid-type N-glycans. (B) Confluent monolayers of MDCK cells were incubated in the absence or presence of DMJ (100 μg/mL) or Sw (2 μg/μL) for 48 h and lysed. Cell lysates were analyzed by immunoblotting using the antibodies against the Na, K-ATPase β_1 subunit. In the absence of inhibitors, the Na,K-ATPase β_1 subunit has two N-glycosylated forms, the mature form (M) and immature form (I). The electrophoretic mobility of the immature form of the Na,K-ATPase β_1 subunit is similar to that of the high-mannose form of the β_1 subunit formed in the presence of DMJ (left panel, H-M) but greater than that of the hybrid-type β_1 subunit formed in the presence of Sw (central panel), indicating that the immature form of the Na,K-ATPase β_1 subunit is high-mannose type but not hybrid type. This high-mannose form of the β_1 subunit is converted into a deglycosylated product by EndoH (right panel, DG). In contrast, the mature fully glycosylated form of the β_1 subunit is resistant to EndoH digestion (right panel), indicating that it contains only complex-type N-glycans.

Expression of Exogenous β Subunits Decreases the Amount of the Complex-Type but Not the High-Mannose Endogenous β_1 Subunits. Expression of YFP-linked rat β_1 subunit decreases the amount of the complex-type endogenous β_1 subunit in the whole cell lysate by 52%, without a significant change in the amount of the α_1 subunit (Figure 2A,B). The amount of the complex-type endogenous β_1 subunit is also decreased with expression of YFP-β_2 and YFP-linked dog β_1 subunit by 47% and 61%, respectively (Figure 2A,B), but not with expression of the P/G mutant of YFP-β_2 that does not interact with the α_1 subunit (see below, Figure 5).

Quantitative PCR shows no significant difference in the amount of mRNA of the endogenous α_1 or β_1 subunit in nontransfected and YFP-β_1-transfected cells (Supporting Information Figure 3), indicating that the decrease of the amount of the endogenous β_1 subunit in the YFP-β_1-expressing cell line is not due to decreased transcription of the gene encoding the β_1 subunit. Also, there is no change in the amount of the ER-located high-mannose endogenous β_1 subunits in the whole cell lysate (Figure 2A,C), showing that translation of the β_1 subunit is not inhibited by expression of exogenous β subunits. The total amount of the ER-located β subunits (endogenous and expressed) is increased in all transfected cells (Figure 2C), consistent with the increase in the total message for the β_1 subunit (endogenous and expressed) due to transfection.

The amount of the α_1 subunit is similar in nontransfected and transfected cells (Figure 2B). The decrease in the complex-type endogenous β_1 subunit is compensated for by expression of the exogenous β subunits, so that the total amount of the complex-type β subunits (endogenous and expressed) is not significantly different from the amount of the complex-type endogenous β_1 subunit in nontransfected cells (Figure 2B). Therefore, the ratio between the total amount of complex-type β subunits and the α_1 subunit is not altered by expression of exogenous β subunits.

Association of YFP-β_1 with the Endogenous α_1 Subunits Decreases the Amount of α_1-Bound Endogenous β_1 Subunits in the ER and in the Basolateral Membrane. To determine whether the exogenous β subunits replace the endogenous β_1 subunit in $\alpha-\beta$ heterodimers, we examined the amount of the α_1-bound endogenous and exogenous β_1 subunits in nontransfected and YFP-β_1-expressing cells. Immunoprecipitation of the α_1 subunit in nontransfected MDCK cells results in coprecipitation of the endogenous β_1 subunit. In YFP-β_1-expressing cells, immunoprecipitation of the α_1 subunit coprecipitates both endogenous β_1 subunits and the added YFP-β_1 subunits (Figure 3A, right panel), indicating that the α_1 subunit associates not only with the endogenous β_1 subunit but also with the expressed YFP-β_1 subunit.

The α_1-coprecipitated fractions of the β_1 subunit and YFP-β_1 contain both complex-type and high-mannose forms (Figure 3A, right panel). The amount of the complex-type endogenous β_1 subunits bound to α_1 subunits is decreased by 48% in YFP-β_1-expressing cells as compared to nontransfected cells (Figure 3A,

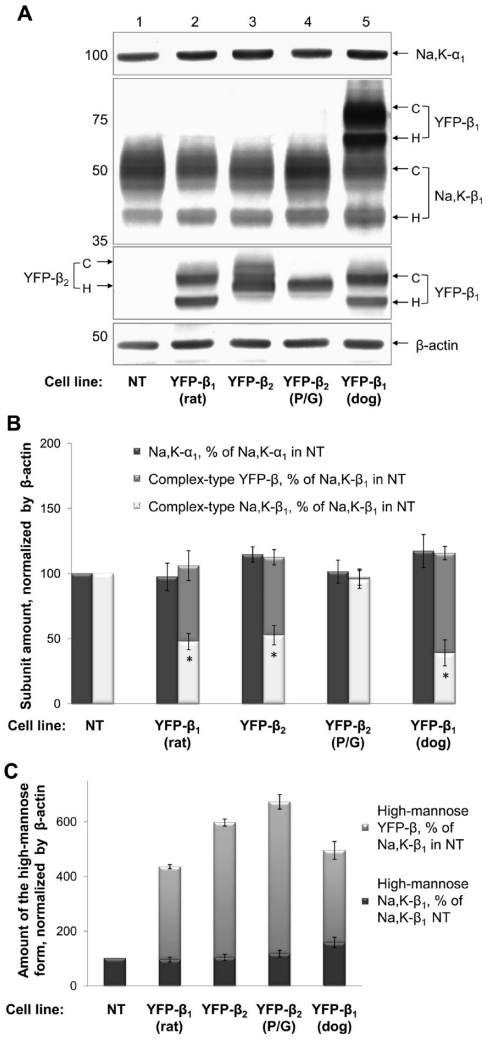

FIGURE 2: Expression of exogenous Na,K-ATPase β subunits significantly decreases the amount of the complex-type endogenous β_1 subunit without a change in the amount of the high-mannose endogenous β_1 subunit in MDCK cells. (A) Equal amounts of whole cell lysates of nontransfected cells and cells expressing various exogenous β subunits were analyzed by SDS−PAGE followed by immunoblotting using the antibodies against the α_1 and β_1 subunits of the Na,K-ATPase, against YFP, and against β-actin. The antibody used for detection of the endogenous canine Na,K-ATPase β_1 subunit does not react with rat YFP-β_1 but does react with dog YFP-β_1. (B, C) Densitometry quantification of the results presented in (A). Quantification of YFP-linked β subunits in cells expressing YFP-β_1 (rat), YFP-β_2, YFP-β_2 (P/G) (lanes 2, 3, and 4 in (A)) relative to the endogenous Na,K-ATPase β_1 subunit in nontransfected cells (lane 1 in (A)) was performed by using a conversion factor equal to the ratio between the density of the YFP-β_1 (dog) band detected by anti-β_1 antibody and the density of the YFP-β_1 (dog) band detected by anti-YFP antibody (lane 5 in (A)). (B) Expression of the wild-type YFP-β_1 (rat), YFP-β_2, and YFP-β_1 (dog) decreases the amount of the complex-type glycosylated form of the endogenous Na,K-ATPase β_1 subunit by 47−61% but does not alter the amount of the Na,K-ATPase α_1 subunit. Expression of the P/G mutant of YFP-β_2 does not alter the amount of either the α_1 or endogenous β_1 subunit. The ratio between the total amount of the Na,K-ATPase β subunit (endogenous and exogenous) and the endogenous α_1 subunit in all transfected cell lines is similar to the ratio between β_1 and α_1 subunits in nontransfected cells. (C) The amount of the high-mannose form of the endogenous β_1 subunit is not altered by expression of the exogenous β subunits. The total amount of the high-mannose subunits (endogenous and exogenous) is significantly increased in all transfected cell lines. Error bars, SD ($n = 3$). *, significant difference with NT, $P < 0.01$, Student's t-test. Key: Na,K-α_1 and Na,K-β_1, the endogenous α_1 and β_1 subunits of the Na,K-ATPase; C, complex-type glycosylated form; H, high-mannose glycosylated form.

right panel, and Figure 3B). A similar decrease in the ratio between the complex-type endogenous β_1 subunits and the α_1 subunits is observed in the whole cell lysate and in the basolateral membrane (Figure 3A,B), suggesting that all complex-type β_1 subunits are bound to the α_1 subunits in nontransfected and transfected cells.

The presence of high-mannose forms in α_1-bound endogenous and exogenous β subunits (Figure 3A, right panel) reflects assembly of $\alpha-\beta$ complexes in the ER, where the β subunits have only high-mannose-type N-glycans. These high-mannose forms comprise 2−3% of the total amount of α_1-bound β_1 subunits (Figure 3A, right panel, and Figure 3C), that likely reflects the relative residence time of the $\alpha-\beta$ complexes in the ER.

The percentage of the high-mannose form of the endogenous β_1 subunit is greater in whole cell lysate than in the α_1-coprecipitated fractions both in nontransfected and in YFP-β_1-expressing cells. Similarly, the percentage of high-mannose YFP-β_1 is greater in the total cell lysate than in the α_1-coprecipitated fractions (Figure 3A, right panel, and Figure 3C). These results indicate that some of the high-mannose ER-resident endogenous and exogenous β_1 subunits are not assembled with α_1 subunits.

A comparison of the percentages of the high-mannose forms in the α_1-coprecipitated fractions and cell lysates shows that 24% of high-mannose β_1 subunits are assembled with the α_1 subunits in nontransfected cells and only 11% of the ER-resident endogenous β_1 subunits are bound to the α_1 subunits in YFP-β_1-expressing cells (Figure 3C). Since the amount of the high-mannose β_1 subunits is similar in transfected and nontransfected cells (Figure 2C), these data show that expression of YFP-β_1 decreases the amount of α_1-bound high-mannose endogenous β_1 subunits in the ER about 2-fold. Consistent with these data, a similar decrease is observed in the amount of the α_1-bound complex-type endogenous β_1 subunits in YFP-β_1-expressing cells as compared to nontransfected cells (Figure 3A, right panel, and Figure 3B).

Therefore, all complex-type, but not all high-mannose-type, endogenous β_1 subunits are assembled with the α_1 subunits in both nontransfected and YFP-β_1-expressing cell lines. Expression of YFP-β_1 decreases the amount of α_1-bound endogenous β_1 subunits approximately by 50% both in the ER and in the basolateral membrane.

The ER-Retained Unassembled β_1 Subunits Are Rapidly Degraded. To determine whether expression of YFP-β_1 affects the degradation rate of the endogenous β_1 subunits, we examined changes of the basolateral and cellular contents of the β_1 subunit during incubation of cells in the presence of the inhibitor of protein synthesis, cycloheximide. The basolateral content of the endogenous β_1 subunit decreases by approximately 15% after 8 h of cell incubation with cycloheximide (Supporting Information Figure 4). A similar decrease is observed for the basolateral α_1 subunit and YFP-β_1 (Supporting Information Figure 4). No significant differences in the rates of decrease of the β_1 subunit are found in transfected and nontransfected cells (Supporting Information Figure 4), indicating that expression of YFP-β_1 does not affect degradation of the plasma membrane β_1 subunits.

Since all complex-type β_1 subunits and only a minor fraction of high-mannose β_1 subunits are α_1-associated, the amount of complex-type and high-mannose forms of the β_1 subunits was quantified in cell lysates during cell incubation with cycloheximide to determine whether the α_1-bound and unassembled β_1 subunits are degraded differently.

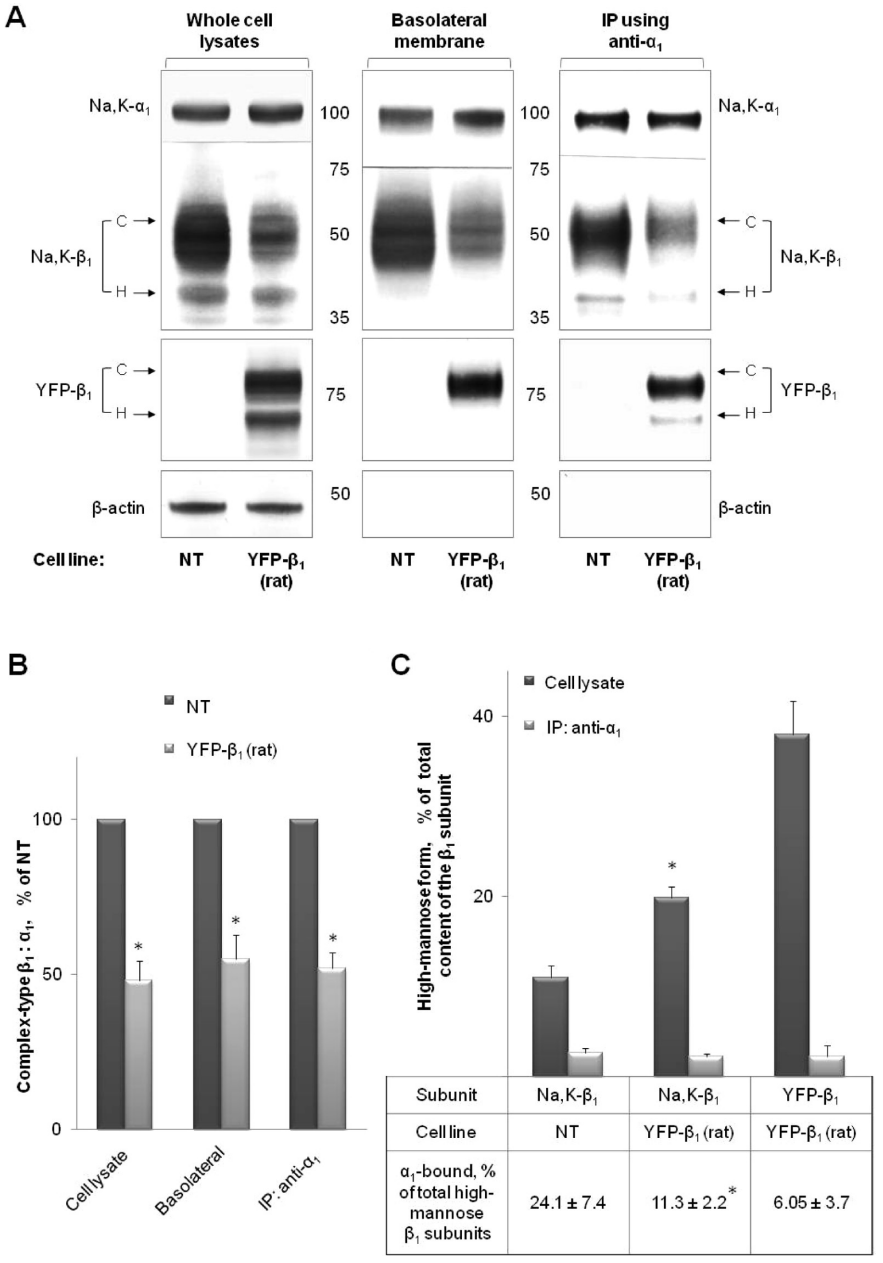

FIGURE 3: Expression of the exogenous β_1 subunit of the Na,K-ATPase decreases the efficiency of the assembly of its high-mannose form with the α_1 subunit. (A) The whole cell lysates, basolateral membrane proteins, and proteins immunoprecipitated using the antibody against the Na,K-ATPase α_1 subunit were obtained from nontransfected MDCK cells and MDCK cells expressing an YFP-linked rat β_1 subunit as described in Materials and Methods. All three protein fractions were analyzed by SDS−PAGE followed by immunoblotting using the antibodies against the Na,K-ATPase α_1 subunit, Na,K-ATPase β_1 subunit, YFP, and β-actin. The antibody used for detection of the endogenous canine Na,K-ATPase β_1 subunit does not react with the rat β_1 subunit of YFP-β_1. The β-actin was used as a loading control in whole cell lysates and as a negative control in basolateral and immunoprecipitated fractions to show no contamination by the nonrelated proteins of the cell lysate. (B, C) Densitometry quantification of the results presented in (A). (B) Expression of YFP-β_1 decreases the ratio between the amount of the complex-type glycosylated form of the endogenous β_1 subunit and the amount of the α_1 subunit in whole cell lysates, basolateral membrane fractions, and α_1-immunoprecipitated fractions by 46−52%. (C) The percentages of the high-mannose forms of both the endogenous Na,K-ATPase β_1 subunit and YFP-β_1 are higher in whole cell lysates than in α_1-immunoprecipitates, showing that only some of the high-mannose subunits are assembled with the α_1 subunit. The fraction of the α_1-bound high-mannose β_1 subunits of total high-mannose β_1 subunits that was calculated as the ratio between percentages of the high-mannose β_1 subunit in α_1-immunoprecipitated fractions and whole cell lysates is decreased by expression of YFP-β_1 (see table). Error bars and errors, SD ($n = 3$). *, significant difference with NT, $P < 0.01$, Student's t-test. Key: Na,K-α_1 and Na,K-β_1, the endogenous α_1 and β_1 subunits of the Na,K-ATPase; C, complex-type glycosylated form; H, high-mannose glycosylated form.

In both nontransfected and YFP-β_1-expressing cell lines, the amount of the complex-type β_1 subunit decreases only slightly after 5 h of incubation with the inhibitor (Figure 4A,B). In contrast, the amount of high-mannose β_1 subunits rapidly decreases during incubation of nontransfected or transfected cells with cycloheximide. Its content is reduced by 50−60% after 1 h (Figure 4A,B). Similarly, the high-mannose YFP-β_1 also is decreased much faster than complex-type YFP-β_1 as seen in Figure 4A.

In nontransfected and YFP-β_1-expressing cell lines, only a minor fraction of the ER-located high-mannose β_1 subunits is assembled with the α_1 subunits as found by precipitation by the

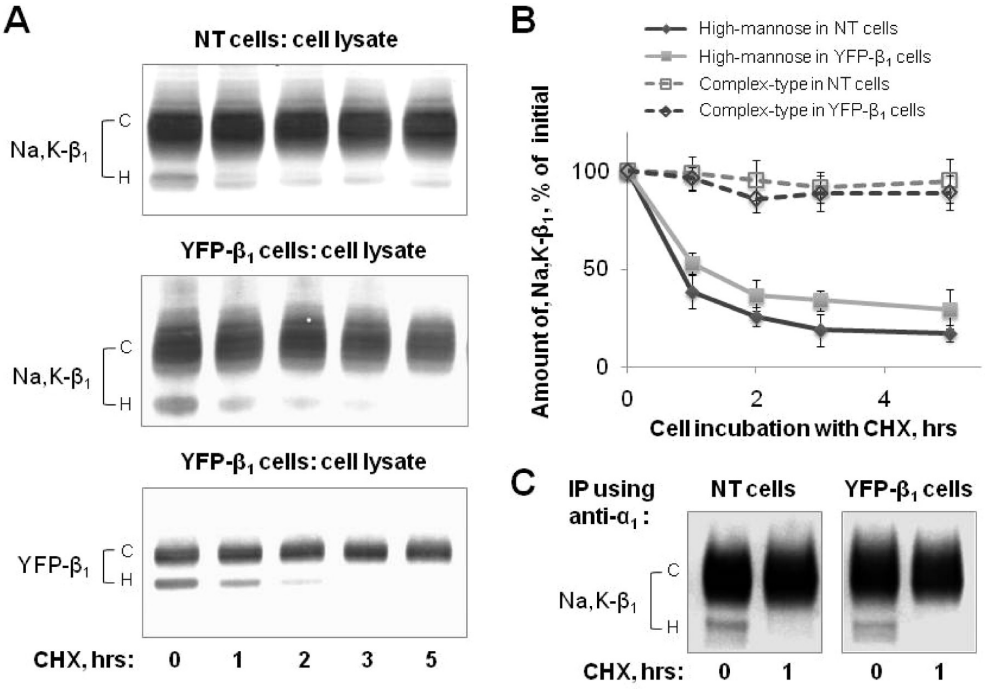

FIGURE 4: High-mannose forms of the endogenous β_1 subunit and YFP-β_1 are degraded more rapidly than the complex-type subunits. (A) Tight monolayers of nontransfected and YFP-β_1-expressing MDCK cells were incubated in the presence of 20 μg/mL cycloheximide (CHX) for the indicated time periods and lysed. Equal volumes of the whole cell lysates were analyzed by Western blot using the antibodies against the Na,K-ATPase β_1 subunit and against YFP. The level of high-mannose forms of both Na,K-ATPase β_1 subunit and YFP-β_1 decreases much more rapidly than the amount of the complex-type forms during 5 h incubation with CHX. (B) Densitometry of the results presented in (A) shows that the amount of complex-type β_1 subunit decreases only by 10% after 5 h incubation with CHX. In contrast, the amount of the high-mannose β_1 subunit decreases by 50−60% after only 1 h incubation. (C) The Na,K-ATPase α_1 subunit was immunoprecipitated from lysates of nontransfected and YFP-β_1-expressing MDCK cells incubated in the absence or presence of CHX for 1 h as described in Materials and Methods. Coprecipitated Na,K-ATPase β_1 subunits were analyzed by Western blot. In the absence of the inhibitor, the α_1-bound β_1 subunits contain a predominant fraction of complex-type and a minor fraction of the high-mannose-type glycoforms in both nontransfected and transfected cells. The high-mannose fraction is not detected after 1 h incubation with CHX in either cell line even after overexposure of the blots (lanes 2). Error bars and errors, SD (n = 3). Key: Na,K-β_1, the endogenous β_1 subunit of the Na,K-ATPase; C, complex-type glycosylated form; H, high-mannose glycosylated form.

anti-α_1 antibody (Figures 3C and 4C). These α_1-bound high-mannose β_1 subunits disappear after 1 h incubation with cycloheximide (Figure 4C), indicating that they are rapidly exported to the Golgi and processed to hybrid and complex type. In contrast, unassembled high-mannose β_1 subunits are not able to traffic from the ER to Golgi. Hence, in the absence of protein synthesis, a decrease in the amount of these high-mannose β_1 subunits reflects mainly the ER-associated degradation (ERAD) of unassembled β_1 subunits. Therefore, the ER-retained unassembled β_1 subunits are degraded much more rapidly than α_1-associated complex-type β_1 subunits.

Mutations in α_1-Interacting Regions of the β_1 and β_2 Subunits Impair $\alpha-\beta$ Association and Result in ER Retention of Unassembled β Subunits. To determine whether binding to the α subunit is necessary for the ER export of the β_2 subunit of the Na,K-ATPase, several point mutations were introduced into known sites of $\alpha-\beta$ interaction in the β_2 subunit. According to the crystal structure of the Na,K-ATPase at 2.4 Å resolution (2ZXE) (*13*), association between the α_1 subunit and the β_1 subunit is supported by interaction between both the extracellular and transmembrane domains of the two subunits (Figure 5A). P245 in the β_1 subunit is adjacent to a stretch of amino acid residues 246YYGK that directly interact with the 7−8 extra-cytoplasmic loop of the α_1 subunit (*13*). Y39, F42, and Y43 interact with the residues in the seventh transmembrane domain of the α_1 subunit (*13*). Mutations of homologous residues were introduced into YFP-β_2, producing P229G (P/G) and Y44A/F47A/Y48A (YFY/AAA) mutants of YFP-β_2 (Supporting Information Figure 1).

The wild-type YFP-β_2 is found mostly in the basolateral membranes of MDCK cells where it is colocalized with the endogenous α_1 subunit (Figure 5C, panel YFP-β_2 (WT)). Antibody against YFP coimmunoprecipitates the endogenous Na,K-ATPase α_1 subunit with YFP-β_2 (Figure 5B, lane WT). These results show that YFP-β_2 is associated with the α_1 subunit.

YFY/AAA and P/G mutations in YFP-β_2 do not alter susceptibility of the subunits to trypsin digestion (Supporting Information Figure 5), indicating that the mutations do not affect overall conformation and folding of the subunit. The YFY/AAA and P/G mutations result in major and full retention of YFP-β_2 inside the cells, respectively (Figure 5C). The mutant YFY/AAA shows incomplete colocalization with the endogenous α_1 subunit (Figure 5C). The P/G mutant of YFP-β_2 shows no colocalization with the α_1 subunit (Figure 5C). No α_1 subunits are detected in the ER (Figure 5C, middle panels). Immunostaining for specific markers of the intracellular compartments indicates that the mutants are partially or completely retained in the ER. Colocalization of the P/G mutant of YFP-β_2 with the ER marker is shown as an example (Figure 5D). The extent of the ER retention detected by confocal microscopy (Figure 5C) correlates with the increase in the relative content of the ER-resident high-mannose form of YFP-β_2 in the mutants (Figure 5B, top panel) and inversely correlates with the efficiency of coimmunoprecipitation of the α_1 subunit with YFP-β_2 (Figure 5B, bottom panel).

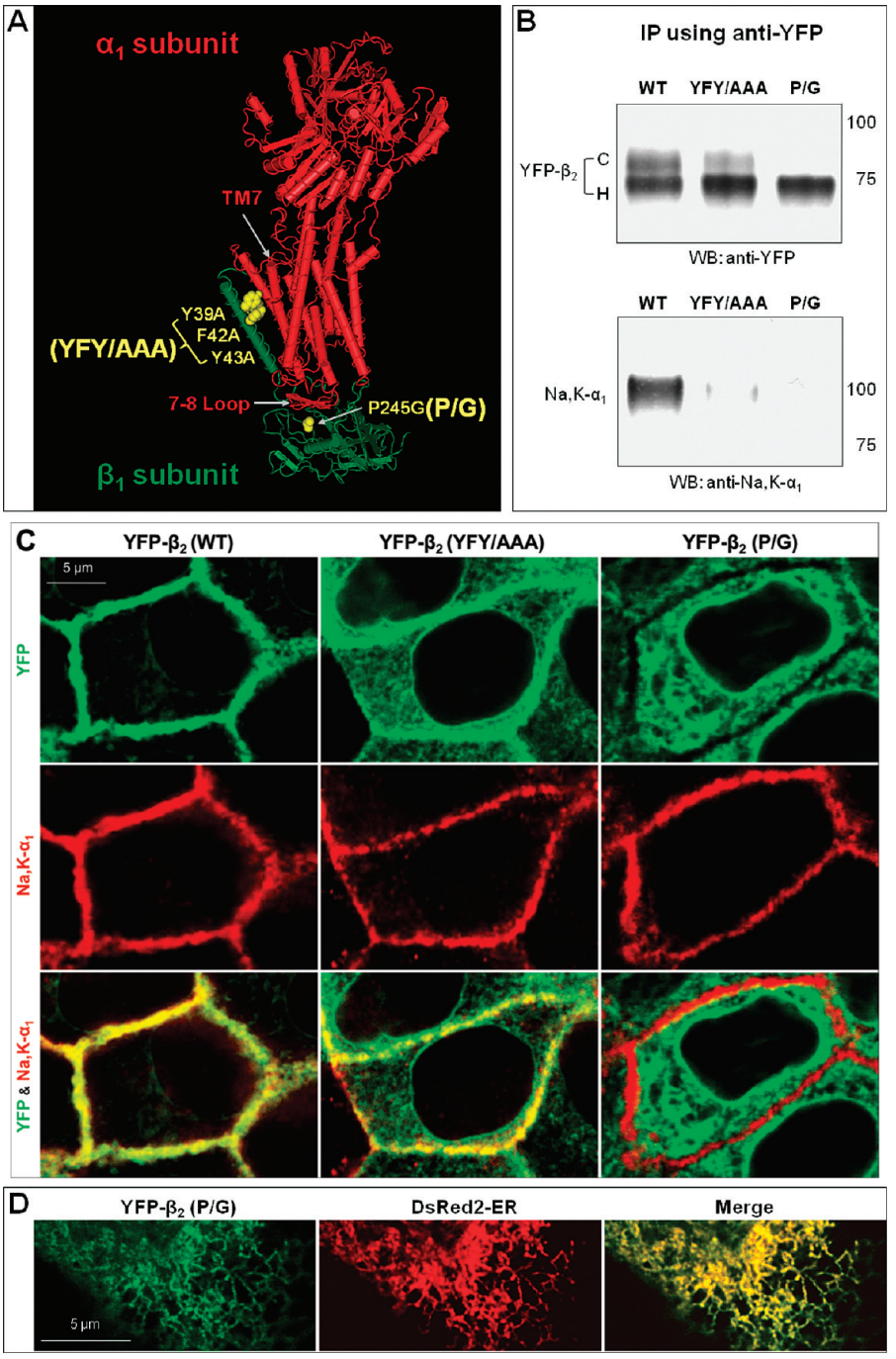

FIGURE 5: Impairment of α−β association due to the point mutations in the α-interacting regions of the β_2 subunit correlates with retention of the mutants in the ER. (A) A model of the Na,K-ATPase α_1 and β_1 subunits based on the crystal structure of the sodium−potassium pump at 2.4 Å resolution (2ZXE) (*13*) shows positions of a triple mutation, Y39A/F42A/Y43A (YFY/AAA), and a single mutation, P245G (P/G), that were introduced into putative α_1-interacting regions of the YFP-linked rat β_1 subunit. The model shows that Y39, F42, and Y43 are located at the interface between the transmembrane domain of the β_1 subunit and the seventh transmembrane domain (TM7) of the α_1 subunit and P245 is located at the interface between the extracellular domain of the β_1 subunit and the 7−8 loop of the α_1 subunit. Numbering of the amino acid residues corresponds to the rat β_1 subunit. The residues homologous to Y39, F42, Y43A, and P245 were also mutated in the YFP-linked human β_2 subunit based on the alignment shown in Supporting Information Figure 1, producing a triple mutant, Y44A/F47A/Y48A (YFY/AAA), and a single mutant, P229G (P/G), of YFP-β_2. (B) The wild-type YFP-β_2 and its YFY/AAA and P/G mutants were immunoprecipitated from the respective cell lysates using the antibody against YFP. Precipitated YFP-linked proteins and coprecipitated endogenous α_1 subunit were analyzed by immunoblotting. The percentage of the high-mannose form of YFP-β_2 is increased in the mutants (top panel). Coimmunoprecipitation of the α_1 subunit with YFP-β_2 is decreased by YFY/AAA mutations and abolished by P/G mutation (bottom panel). (C) Immunostaining of the endogenous α_1 subunit shows that the wild-type YFP-β_2 precisely colocalizes, the YFY/AAA mutant only partially colocalizes, and the P/G mutant does not colocalize with the α_1 subunit in the basolateral membrane. (D) Transient transfection of cells expressing the P/G mutant of YFP-β_2 with the fluorescent marker of the ER, DsRed2-ER, shows colocalization of the mutant and the ER. Key: Na,K-α_1, the endogenous α_1 subunit of the Na,K-ATPase; C, complex-type glycosylated form; H, high-mannose glycosylated form.

Homologous mutations in YFP-β_1, Y39A/F42A/Y43A and P245G, also impair α−β association and increase the ER retention of unassembled mutants without affecting protein folding (not shown).

DISCUSSION

Only α-Assembled Na,K-ATPase β Subunits Can Exit the ER. It is well established that the Na,K-ATPase α_1 subunit is unable to exit the ER unless it is assembled with the β subunit in various expression systems (*14*). Equally, the results presented in this paper demonstrate that assembly with the α_1 subunit is also required for the export of either β_1 or β_2 subunit from the ER in MDCK cells.

The dependence of the export of the β_2 subunit from the ER to Golgi on the α_1 subunit association is shown by the results of site-directed mutagenesis of the β_2 subunit in the two regions of its specific interaction with the α_1 subunit. Both the YFY/AAA mutation in the transmembrane domain and the P/G mutation in the extracellular domain of the β_2 subunit partially or completely disrupt $\alpha-\beta$ association as determined by loss in both coimmunoprecipitation and microscopic colocalization of YFP-β_2 and α_1 subunit (Figure 5B,C) without affecting protein folding as assessed by susceptibility of the mutants to trypsin digestion (Supporting Information Figure 5). Proportionately to the degree of impairment of $\alpha-\beta$ association, unassembled mutants are partially or completely retained in the ER as detected by colocalization with an ER marker (Figure 5D) and by the quantitative increase in the relative content of the ER-resident high-mannose form of the β subunits (Figure 5B, top panel). Therefore, association with the α_1 subunit is required for export of the β_2 subunit from the ER.

Homologous mutations in YFP-β_1 also impair $\alpha-\beta$ association and increase ER retention of unassembled mutants, confirming previously published data on inability of the unassembled β_1 subunit to traffic from the ER to Golgi (*10*, *24*−*26*). Additional evidence is presented here by comparing the effects of expression of the YFP-linked rat β_1 subunit on the amount of the endogenous Na,K-ATPase subunits in different cellular fractions. Transfection decreases the ratio between the amount of the endogenous complex-type β_1 subunit and amount of the α_1 subunit to the same extent in the whole cell lysate, basolateral membrane, and α_1-immunoprecipitated fractions (Figure 3A,B). These data demonstrate that all complex-type β_1 subunits are assembled with the α_1 subunit in both nontransfected and transfected cells. The alternative possibility that the unassembled β_1 subunits are delivered to the plasma membrane but are rapidly endocytosed and degraded in transfected cells is ruled out by the experiments showing the same rate of degradation of the plasma membrane resident Na,K-ATPase subunits in both transfected and nontransfected cells (Supporting Information Figure 4).

As for the Na,K-ATPase β_1 and β_2 subunits, the Na,K-ATPase β_3 subunit requires assembly with the α subunit to exit the ER (*24*−*26*). Therefore, the inability to exit the ER without α-association is a property common to all three Na,K-ATPase β subunit isoforms. In contrast, the homologous H,K-ATPase β subunit is able to reach the plasma membrane when expressed without the H,K-ATPase α subunit in various cell types (*28*−*32*). This ability to exit the ER, at least in part, can be explained by association of the H,K-ATPase β subunit with the endogenous Na,K-ATPase α subunit (*32*). However, the presence of the expressed H,K-ATPase β subunit and the absence of the endogenous Na,K-ATPase α subunit in the apical membranes of polarized MDCK and LLC-PK1 cells show that a fraction of the H,K-ATPase β subunits is able to exit the ER without the α subunits (*30*−*32*). The efficiency of the ER export of the H,K-ATPase β subunit is greatly increased by coexpression of the H,K-ATPase α subunit (*36*), suggesting that plasma membrane trafficking of the unassembled β subunit is due to a "leak" of the ER quality control system. One of the possible reasons for this difference of the H,K-ATPase β subunit from homologous Na,K-ATPase β subunits might be lack of interaction of the H,K-ATPase β subunit with BiP (*26*), the ER chaperone responsible for the ER retention of unassembled subunits of many oligomeric proteins, including the Na,K-ATPase subunits (*26*). It is also possible that α-unassembled H,K-ATPase and Na,K-ATPase β subunits differ from each other in binding affinity to the ER lectins facilitating the ER to Golgi trafficking.

The ER Quality Control System Imposes an Equimolar Ratio between Na,K-ATPase α and β Subunits in the Plasma Membrane. Expression of rat YFP-β_1 significantly decreases the amount of the endogenous β_1 subunit but does not alter the amount of the α_1 subunit (Figures 2 and 3) or mRNA level of either subunit (Supporting Information Figure 3) or degradation of the plasma membrane resident subunits (Supporting Information Figure 4).

Similar to our data, expression of flag-conjugated sheep β_1 subunit in MDCK cells did not alter mRNA level of endogenous subunits or the amount of the α_1 subunit but decreased the level of the endogenous β_1 subunit (*37*). Based on these results, the authors concluded that translation of the endogenous β_1 subunit is repressed by expression of the exogenous β_1 subunit by an unknown mechanism (*37*).

However, separate detection and quantification of the complex-type and high-mannose forms of the endogenous β_1 subunit as performed here favor a different interpretation of these results. We find that only the complex-type fraction of the endogenous β_1 subunit is reduced due to expression of exogenous β subunits, but the amount of the high-mannose, ER-resident, form does not change (Figure 2), implying that translation of the endogenous β_1 subunit is not repressed by exogenous β subunits. The presence of exogenous YFP-β_1 decreases the amount of the α_1-bound endogenous β_1 subunits both in the ER (Figure 3C) and in the basolateral membrane (Figure 3B) by approximately 50%. The amount of the α_1 subunit does not change, while the complex-type YFP-β_1 compensates for the decrease in the complex-type endogenous β_1 subunit (Figure 2B). These data show that expressed YFP-β molecules compete with the endogenous β_1 subunits for a limited number of the α_1 subunits in the ER and replace the endogenous subunits in about half of the newly formed $\alpha-\beta$ complexes. Only assembled $\alpha-\beta$ complexes are exported from the ER to Golgi, while the unassembled β subunits are retained in the ER and degraded through the ER-associated degradation (ERAD) pathway. The ER-retained unassembled β_1 subunits are degraded much more rapidly than the α_1-bound complex-type β_1 subunits in both transfected and nontransfected cell lines (Figure 4), which can explain why a 50% decrease in the α_1-bound endogenous β_1 subunits is not accompanied by an equivalent increase in the amount of the ER-retained unassembled endogenous β_1 subunits (Figure 2). Therefore, a decrease in the abundance of the endogenous β_1 subunit by expression of exogenous β subunits, as shown here (Figures 2 and 3) and previously (*37*), is likely due to competition of the β subunits for association with the limited number of the α_1 subunits and rapid degradation of the ER-retained unassembled β subunits. This explanation is more straightforward than translational repression (*37*). In agreement with our interpretation, expression of the P/G mutant of YFP-β_2 that is not able to assemble with the endogenous Na,K-ATPase α_1 subunit does not change the

amount of the endogenous β_1 subunits (Figure 2). Similarly, the β_1/β_2 chimera that is not associated with the α_1 subunit does not affect the amount of the endogenous β_1 subunits in MDCK cell subunits (*37*).

Only 24% of high-mannose β_1 subunits are bound to α_1 subunits (Figure 3C). The unassembled β_1 subunits are degraded faster than α-bound subunits (Figure 4). These data imply that less than a quarter of the newly synthesized β_1 subunits assemble with the α_1 subunit. Consistently, pulse−chase experiments show that β_1 subunits are synthesized in 5:1 excess over the α_1 subunit in MDCK cells (*38*). The newly synthesized immature β_1 subunits are rapidly degraded, and only after 60 min, which coincides in time with maturation of the β_1 subunits, are the α_1 and β_1 subunits detected with a 1:1 stoichiometry (*38*). Therefore, the number of α_1 subunits in the ER appears to be the limiting factor that determines the number of $\alpha_1-\beta_1$ complexes in MDCK cells.

Expression of the wild-type YFP-β_1 (rat or dog) or YFP-β_2 results only in an insignificant change of both the α_1 subunit and total amount of the mature Na,K-ATPase β subunits (endogenous and exogenous), so that the ratio between the total amount of complex-type β subunits and α_1 subunits remains constant (Figure 2). These data indicate that, similar to the endogenous β subunits, the exogenous β subunits form equimolar complexes with the endogenous α_1 subunits.

It is likely that the ER quality control that allows export only of assembled $\alpha-\beta$ complexes is a common mechanism that ensures a 1:1 ratio between α and β subunits in the plasma membranes of all animal cells. In most cells, rapid degradation of unassembled subunits via ERAD maintains this ratio close to one also in intracellular membranes. Indeed, the equimolar ratio between α and β subunits was found not only in purified Na, K-ATPase preparations but also in total microsome membrane fractions in many different cell types, including renal, liver, and brain cells (*39*−*42*). However, in certain cells, such as the *Xenopus* oocytes and rat cardiac myocytes, the α subunit is present in an excess in intracellular membrane fractions (*43*, *44*). In *Xenopus* oocytes, the functioning $\alpha-\beta$ complexes are expressed in the plasma membrane, while a significant amount of unassembled α subunits is accumulated in the ER (*43*). In cardiac myocytes, the majority of the active pumps containing α and β subunits at 1:1 stoichiometry is detected in caveolae, and a 5-fold excess of the α subunits over β subunits is found in caveolin-free membrane fractions (*44*). The majority of caveolin-free fractions contain ER markers implying that this excess of the α subunit is mostly due to the ER retention of unassembled α subunits. In addition, it is possible that two subunits of the Na,K-ATPase might disassemble after internalization and undergo distinct endocytic and degradation pathways, as the authors suggested based on unequal ratios between the α and β subunits detected in early and late endosomal fractions (*44*).

Only the α-Bound β Subunits Modulate Intercellular Adhesion and Cell Migration. Both the β_1 and β_2 subunits play important roles in intercellular adhesion and cell migration. The Na,K-ATPase β_2 subunit was first described as an adhesion protein in glial cells (AMOG) that mediates neuron−astrocyte interaction and neuron migration (*17*, *18*). Overexpression of the Na,K-ATPase β_1 subunit in nonpolarized CHO cells facilitates formation of intercellular junctions (*21*). The β_1 subunit of the Na,K-ATPase is necessary for formation and stabilization of adherens junctions in MDCK cells (*19*, *23*). The Na,K-ATPase β_1 subunit is also involved in regulation of cell motility (*20*). Both the tightness of intercellular junctions and cell motility depend on the extent of N-glycan branching of the Na,K-ATPase β_1 subunit (*22*). Furthermore, formation of tight cell monolayers from relatively motile dispersed MDCK cells is accompanied by changes in the level of expression of specific glycosyltransferases that result in a gradual decrease in N-glycan branching (*22*), suggesting that intercellular adhesion and cell migration are regulated via glycosyltransferase-mediated remodeling of N-glycans of the Na,K-ATPase β subunit.

The evidence presented here on the absence of unassembled β subunits in the plasma membrane indicates that both β_1 and β_2 subunits can regulate cell adhesion and migration only as components of the $\alpha-\beta$ complexes. Therefore, the adhesive function of the β subunits cannot be modulated independently of ion transport activity by altering β subunit abundance on the cell surface. However, cells can regulate cell adhesion and/or migration by remodeling of the structure of N-glycans of the β subunits without affecting the quantity and, hence, activity of the pump.

In conclusion, the relative amounts of the Na,K-ATPase subunits in the plasma membrane of MDCK cells is tightly regulated. The ER quality control system allows export of only equimolar $\alpha-\beta$ complexes to the Golgi, thus ensuring that no unassembled subunits are present in the plasma membrane. The number of the pumps in the membrane is determined by the amount of the α subunit in the ER, the limiting factor for the formation of $\alpha-\beta$ complexes.

ACKNOWLEDGMENT

The authors are thankful to Dr. Liora Shoshani for providing the cDNA encoding the dog Na,K-ATPase β_1 subunit.

SUPPORTING INFORMATION AVAILABLE

Tables 1 and 2 and Figures 1−5 as described in the text. This material is available free of charge via the Internet at http://pubs.acs.org.

REFERENCES

1. Xie, Z. (2003) Molecular mechanisms of Na/K-ATPase-mediated signal transduction. *Ann. N.Y. Acad. Sci. 986*, 497–503.
2. Tian, J., and Xie, Z. J. (2008) The Na-K-ATPase and calcium-signaling microdomains. *Physiology* (*Bethesda, MD*) *23*, 205–211.
3. Blanco, G., and Mercer, R. W. (1998) Isozymes of the Na-K-ATPase: heterogeneity in structure, diversity in function. *Am. J. Physiol. 275*, F633–650.
4. Crambert, G., Hasler, U., Beggah, A. T., Yu, C., Modyanov, N. N., Horisberger, J. D., Lelievre, L., and Geering, K. (2000) Transport and pharmacological properties of nine different human Na, K-ATPase isozymes. *J. Biol. Chem. 275*, 1976–1986.
5. Sweadner, K. J., and Rael, E. (2000) The FXYD gene family of small ion transport regulators or channels: cDNA sequence, protein signature sequence, and expression. *Genomics 68*, 41–56.
6. Craig, W. S., and Kyte, J. (1980) Stoichiometry and molecular weight of the minimum asymmetric unit of canine renal sodium and potassium ion-activated adenosine triphosphatase. *J. Biol. Chem. 255*, 6262–6269.
7. Peterson, G. L., and Hokin, L. E. (1981) Molecular weight and stoichiometry of the sodium- and potassium-activated adenosine triphosphatase subunits. *J. Biol. Chem. 256*, 3751–3761.
8. Brotherus, J. R., Jacobsen, L., and Jorgensen, P. L. (1983) Soluble and enzymatically stable ($Na^+ + K^+$)-ATPase from mammalian kidney consisting predominantly of protomer alpha beta-units. Preparation, assay and reconstitution of active Na^+, K^+ transport. *Biochim. Biophys. Acta 731*, 290–303.
9. Kyte, J. (1971) Purification of the sodium- and potassium-dependent adenosine triphosphatase from canine renal medulla. *J. Biol. Chem. 246*, 4157–4165.

10. Clifford, R. J., and Kaplan, J. H. (2008) beta-Subunit overexpression alters the stoichiometry of assembled Na-K-ATPase subunits in MDCK cells. *Am. J. Physiol. Renal Physiol. 295*, F1314–1323.
11. Yoshimura, S. H., Iwasaka, S., Schwarz, W., and Takeyasu, K. (2008) Fast degradation of the auxiliary subunit of Na^+/K^+-ATPase in the plasma membrane of HeLa cells. *J. Cell Sci. 121*, 2159–2168.
12. Morth, J. P., Pedersen, B. P., Toustrup-Jensen, M. S., Sorensen, T. L., Petersen, J., Andersen, J. P., Vilsen, B., and Nissen, P. (2007) Crystal structure of the sodium-potassium pump. *Nature 450*, 1043–1049.
13. Shinoda, T., Ogawa, H., Cornelius, F., and Toyoshima, C. (2009) Crystal structure of the sodium-potassium pump at 2.4 Å resolution. *Nature 459*, 446–450.
14. Noguchi, S., Mishina, M., Kawamura, M., and Numa, S. (1987) Expression of functional ($Na^+ + K^+$)-ATPase from cloned cDNAs. *FEBS Lett. 225*, 27–32.
15. Geering, K. (2001) The functional role of beta subunits in oligomeric P-type ATPases. *J. Bioenerg. Biomembr. 33*, 425–438.
16. Geering, K. (2008) Functional roles of Na,K-ATPase subunits. *Curr. Opin. Nephrol. Hypertens. 17*, 526–532.
17. Antonicek, H., Persohn, E., and Schachner, M. (1987) Biochemical and functional characterization of a novel neuron-glia adhesion molecule that is involved in neuronal migration. *J. Cell Biol. 104*, 1587–1595.
18. Gloor, S., Antonicek, H., Sweadner, K. J., Pagliusi, S., Frank, R., Moos, M., and Schachner, M. (1990) The adhesion molecule on glia (AMOG) is a homologue of the beta subunit of the Na,K-ATPase. *J. Cell Biol. 110*, 165–174.
19. Rajasekaran, S. A., Palmer, L. G., Quan, K., Harper, J. F., Ball, W. J., Jr., Bander, N. H., Peralta Soler, A., and Rajasekaran, A. K. (2001) Na,K-ATPase beta-subunit is required for epithelial polarization, suppression of invasion, and cell motility. *Mol. Biol. Cell 12*, 279–295.
20. Barwe, S. P., Anilkumar, G., Moon, S. Y., Zheng, Y., Whitelegge, J. P., Rajasekaran, S. A., and Rajasekaran, A. K. (2005) Novel role for Na,K-ATPase in phosphatidylinositol 3-kinase signaling and suppression of cell motility. *Mol. Biol. Cell 16*, 1082–1094.
21. Shoshani, L., Contreras, R. G., Roldan, M. L., Moreno, J., Lazaro, A., Balda, M. S., Matter, K., and Cereijido, M. (2005) The polarized expression of Na^+,K^+-ATPase in epithelia depends on the association between beta-subunits located in neighboring cells. *Mol. Biol. Cell 16*, 1071–1081.
22. Vagin, O., Tokhtaeva, E., Yakubov, I., Shevchenko, E., and Sachs, G. (2008) Inverse correlation between the extent of N-glycan branching and intercellular adhesion in epithelia. Contribution of the Na, K-ATPase beta1 subunit. *J. Biol. Chem. 283*, 2192–2202.
23. Vagin, O., Tokhtaeva, E., and Sachs, G. (2006) The role of the beta1 subunit of the Na,K-ATPase and its glycosylation in cell-cell adhesion. *J. Biol. Chem. 281*, 39573–39587.
24. Ackermann, U., and Geering, K. (1990) Mutual dependence of Na, K-ATPase alpha- and beta-subunits for correct posttranslational processing and intracellular transport. *FEBS Lett. 269*, 105–108.
25. Jaunin, P., Horisberger, J. D., Richter, K., Good, P. J., Rossier, B. C., and Geering, K. (1992) Processing, intracellular transport, and functional expression of endogenous and exogenous alpha-beta 3 Na, K-ATPase complexes in *Xenopus* oocytes. *J. Biol. Chem. 267*, 577–585.
26. Beggah, A., Mathews, P., Beguin, P., and Geering, K. (1996) Degradation and endoplasmic reticulum retention of unassembled alpha- and beta-subunits of Na,K-ATPase correlate with interaction of BiP. *J. Biol. Chem. 271*, 20895–20902.
27. Noguchi, S., Higashi, K., and Kawamura, M. (1990) A possible role of the beta-subunit of (Na,K)-ATPase in facilitating correct assembly of the alpha-subunit into the membrane. *J. Biol. Chem. 265*, 15991–15995.
28. Horisberger, J. D., Jaunin, P., Reuben, M. A., Lasater, L. S., Chow, D. C., Forte, J. G., Sachs, G., Rossier, B. C., and Geering, K. (1991) The H,K-ATPase beta-subunit can act as a surrogate for the beta-subunit of Na,K-pumps. *J. Biol. Chem. 266*, 19131–19134.
29. Jaunin, P., Jaisser, F., Beggah, A. T., Takeyasu, K., Mangeat, P., Rossier, B. C., Horisberger, J. D., and Geering, K. (1993) Role of the transmembrane and extracytoplasmic domain of beta subunits in subunit assembly, intracellular transport, and functional expression of Na,K-pumps. *J. Cell Biol. 123*, 1751–1759.
30. Gottardi, C. J., and Caplan, M. J. (1993) Molecular requirements for the cell-surface expression of multisubunit ion-transporting ATPases. Identification of protein domains that participate in Na,K-ATPase and H,K-ATPase subunit assembly. *J. Biol. Chem. 268*, 14342–14347.
31. Vagin, O., Turdikulova, S., and Sachs, G. (2004) The H,K-ATPase beta subunit as a model to study the role of N-glycosylation in membrane trafficking and apical sorting. *J. Biol. Chem. 279*, 39026–39034.
32. Vagin, O., Turdikulova, S., Yakubov, I., and Sachs, G. (2005) Use of the H,K-ATPase beta subunit to identify multiple sorting pathways for plasma membrane delivery in polarized cells. *J. Biol. Chem. 280*, 14741–14754.
33. Vagin, O., Turdikulova, S., and Sachs, G. (2005) Recombinant addition of N-glycosylation sites to the basolateral Na,K-ATPase beta1 subunit results in its clustering in caveolae and apical sorting in HGT-1 cells. *J. Biol. Chem. 280*, 43159–43167.
34. Gottardi, C. J., Dunbar, L. A., and Caplan, M. J. (1995) Biotinylation and assessment of membrane polarity: caveats and methodological concerns. *Am. J. Physiol. 268*, F285–295.
35. Kroepfl, J. F., and Gardinier, M. V. (2001) Identification of a basolateral membrane targeting signal within the cytoplasmic domain of myelin/oligodendrocyte glycoprotein. *J. Neurochem. 77*, 1301–1309.
36. Vagin, O., Turdikulova, S., and Tokhtaeva, E. (2007) Polarized membrane distribution of potassium-dependent ion pumps in epithelial cells: different roles of the N-glycans of their beta subunits. *Cell Biochem. Biophys. 47*, 376–391.
37. Clifford, R. J., and Kaplan, J. H. (2009) Regulation of Na,K-ATPase subunit abundance by translational repression. *J. Biol. Chem.* (in press).
38. Mircheff, A. K., Bowen, J. W., Yiu, S. C., and McDonough, A. A. (1992) Synthesis and translocation of Na(+)-K(+)-ATPase alpha- and beta-subunits to plasma membrane in MDCK cells. *Am. J. Physiol. 262*, C470–C483.
39. Shanbaky, N. M., and Pressley, T. A. (1995) Transfection of Na, K-ATPase alpha-subunit: regulation of enzyme abundance. *Biochem. Cell Biol. 73*, 261–268.
40. Therien, A. G., Nestor, N. B., Ball, W. J., and Blostein, R. (1996) Tissue-specific versus isoform-specific differences in cation activation kinetics of the Na,K-ATPase. *J. Biol. Chem. 271*, 7104–7112.
41. Sun, Y., and Ball, W. J., Jr. (1992) Determination of Na(+)-K(+)-ATPase alpha- and beta-isoforms and kinetic properties in mammalian liver. *Am. J. Physiol. 262*, C1491–C1499.
42. Jorgensen, P. L. (1980) Sodium and potassium ion pump in kidney tubules. *Physiol. Rev. 60*, 864–917.
43. Geering, K., Theulaz, I., Verrey, F., Hauptle, M. T., and Rossier, B. C. (1989) A role for the beta-subunit in the expression of functional Na^+-K^+-ATPase in *Xenopus* oocytes. *Am. J. Physiol. 257*, C851–C858.
44. Liu, L., and Askari, A. (2006) Beta-subunit of cardiac Na^+-K^+-ATPase dictates the concentration of the functional enzyme in caveolae. *Am. J. Physiol. Cell Physiol. 291*, C569–578.